

PROCEEDINGS OF SPIE

[SPIDigitalLibrary.org/conference-proceedings-of-spie](https://spiedigitallibrary.org/conference-proceedings-of-spie)

Time-multiplexed optical systems for reservoir computing and coherent Ising machines

Van der Sande, Guy, Böhm, Fabian, Harkhoe, Krishan, Pauwels, Jaël, Bienstman, Peter, et al.

Guy Van der Sande, Fabian Böhm, Krishan Harkhoe, Jaël Pauwels, Peter Bienstman, Thomas Van Vaerenbergh, Guy Verschaffelt, "Time-multiplexed optical systems for reservoir computing and coherent Ising machines," Proc. SPIE 11804, Emerging Topics in Artificial Intelligence (ETAI) 2021, 118041Q (2 September 2021); doi: 10.1117/12.2594700

SPIE.

Event: SPIE Nanoscience + Engineering, 2021, San Diego, California, United States

Time-multiplexed optical systems for reservoir computing and coherent Ising machines

Guy Van der Sande^a, Fabian Böhm^a, Krishan Harkhoe^a, Jaël Pauwels^a, Peter Bienstman^b, Thomas Van Vaerenbergh^c, and Guy Verschaffel^a

^aApplied Physics Research Group, Vrije Universiteit Brussel, Pleinlaan 2, 1050 Brussels, Belgium

^bPhotonics Research Group, Department of Information Technology, Ghent University-IMEC, Technologiepark Zwijnaarde 126, 9052 Ghent, Belgium

^cHewlett Packard Labs, 940 North McCarthy Blvd, Milpitas, CA 95035, USA

ABSTRACT

Multiple photonic systems show great promise for providing practical yet powerful hardware substrates for neuromorphic computing. Among those, delay-based systems offer -through a time-multiplexing technique - a simple technological implementation route. We discuss our advances in the development of passive coherent fibre-ring cavities and semiconductor lasers with integrated delay for reservoir computing. Time-multiplexed systems are also highly suitable for coherent Ising machines as they allow to implement a fully interconnected large scale system with few components. We have recently proposed a system based on opto-electronic oscillators subjected to self-feedback with improved calculation time and solution quality.

Keywords: neuromorphic computing, reservoir computing, delayed feedback, semiconductor laser, photonic integration, Ising machines, combinatorial optimization

1. TIME MULTIPLEXING FOR INTEGRATED RESERVOIR COMPUTERS

Artificial neural networks (ANN) have played a significant role in the current AI boom, especially with the invention of ImageNet¹ as catalyst. ANNs may be efficient and versatile during operation, nevertheless they require complex and time-consuming algorithms to train the connection weights in the large network that forms the ANN. When interested in processing tasks and data where the temporal evolution is key, standard feed-forward ANNs are not sufficient and one needs to turn to recurrent neural networks (RNNs). The training of RNNs is a nonlinear problem due to feedback loops in the network and is far more involved than the training algorithms of feed-forward networks. Reservoir computing (RC) is paradigm that solves the training issue of RNNs in an efficient way.

RC offers a framework to exploit the transient dynamics within a RNN for performing useful computation. It has been demonstrated to have state-of-the-art performance for a range of tasks that are notoriously hard to solve by algorithmic approaches, e.g., speech and pattern recognition and nonlinear control. RC simplifies the training procedure for RNNs considerably. Its training procedure only acts on the output layer which consists of a linear combination of network states to generate the desired output signals. The connections of the RNN itself, which is now referred to as reservoir, remain fixed. During training, only the connections from the network to the output layer are adjusted. Due to this simplification, RC is very suited as framework for neuromorphic computing activities in photonics. Today, multiple photonic RC systems exist that can provide a practical yet powerful hardware substrate for neuromorphic computing.² Some examples include a network of semiconductor optical amplifiers, an integrated passive silicon circuit forming a very complex and random interferometer, with nonlinearity introduced in the readout stage and a semiconductor laser network based on diffractive coupling.^{2,3} All these implementations have one thing in common: they rely on a network of photonic nodes that are spatially distributed and can be measured simultaneously.

Further author information: (Send correspondence to GVDS)

GVDS: E-mail: guy.van.der.sande@vub.be

However, the reservoir is not required to be a networked structure. In fact, any dynamical system with a high dimensional state space can be considered as reservoir substrate. We consider here specifically a semiconductor laser with delayed feedback as reservoir substrate. The concept of delay-based RC, using only a single nonlinear node with delayed feedback, was introduced some years ago by Appeltant *et al.*⁴ Delay-based RC offers a simple technological route to implement photonic neuromorphic computation. Its operation boils down to a time-multiplexing with the delay arising from propagation in the external feedback loop, limiting the resulting processing speed. The system is easily scaled by tuning the delay length and only has one single physical node reducing the hardware complexity in photonic systems. The first working prototype was developed in electronics in 2011 by Appeltant *et al.* and studied many configurations.⁵ Several performant optical systems followed quickly after that.⁶⁻⁸ Brunner *et al.*^{9,10} employed of-the-shelf telecom equipment to experiment with a single-mode semiconductor laser subjected to optical feedback. The delay time in his experiments was around 80ns, which translates to a few meters of fiber. As most optical setups end up to be bulky employing long fiber loops or free-space optics, the processing speeds are limited in the range of kSa/s to tens of MSa/s.^{7,9} To increase the processing speed of delay-based reservoir computing using a semiconductor laser with delayed optical feedback, one can integrate the laser and the delay both on the same photonic chip. In this way, by using a waveguide structure with a compact footprint, an external cavity structure can be implemented which is small enough to reach high processing speeds, yet still long enough to have sufficient dimensionality for good computing performance. In the long term, this integrated approach will lead to a robust and low-cost design. Recently, Takano *et al.*¹¹ have presented a photonic integrated circuit consisting of a distributed-feedback semiconductor laser, a semiconductor optical amplifier (SOA), a phase modulator, a short passive waveguide, and an external mirror for optical feedback. The external cavity length in this system reached 10.6mm, corresponding to a round-trip delay time of 254ps. However, only six virtual nodes could be stored within the delay line with node-spacings of 40 ps, not enough for good computational performance. This necessitated the authors to use masks with duration of multiple delay times, which slows down the computation speed. Several other types of semiconductor laser have been considered such as semiconductor ring lasers using the two available directional modes¹² and vertical-cavity surface-emitting employing the two polarization modes^{13,14} and multi-mode lasers employing longitudinal modes.¹⁵ In this paper, we will only focus on single-mode Fabry-Pérot type quantum-well semiconductor lasers.

The information processing performance of a semiconductor laser-based RC system is related to its dynamical behaviour both in the absence of external input and in the presence of said input. After the very first experiment by Brunner *et al.*,⁹ other works have focused on understanding the fundamental properties of semiconductor laser-based RC for non-linear prediction tasks. In Ref. 16, it has been shown that the conditions to achieve good predictive performance are given by the injection locking, consistency, and memory properties of the system. More specifically, Bueno *et al.* found that the lowest prediction error for a non-linear prediction task occurs at the injection locking boundary. Note that in this work the laser was operating below or close to the solitary lasing threshold. Consistency, the ability of a system to have a similar response for the similar input signals, is widely regarded as key for good reservoir computing performance.^{16,17}

Our goal is to show that a delay-based reservoir computer can be built using an indium-phosphide PIC, that combines active and passive elements and is built on the JePPIX platform.¹⁸ The PIC integrates a semiconductor laser with an external cavity of 5.4 cm, which corresponds to a round trip time of 1170 ps. This allows for 23 nodes and a processing speed of 0.87 GSa/s. The longer waveguide based external cavity will also have more loss associated to it. Therefore, we will address in this work the question if amplification in the external cavity is needed or not. Contrary to other works,^{9,11,16} the semiconductor laser itself will be driven far above solitary lasing threshold to benefit from a better signal to noise ratio in the read-out, as well as faster internal dynamics. Finally, we will introduce post-processing schemes that do not penalize computational speed

A schematic of our integrated device is shown in Fig. 1. It consists of a distributed Bragg reflector (DBR) laser structure and two spiral waveguides comprising the delay line. Two semiconductor optical amplifiers (SOA) are placed along the delay line to tune the feedback strength. A phase modulator is available to tune the feedback phase. We have not used this phase modulator due to setup complexity. Nevertheless, the phase is expected to play an important role.¹⁹ At the end of the delay line a DBR element completes the feedback loop by reflection. This on-chip feedback loop has a round-trip time of $\tau = 1170$ ps.

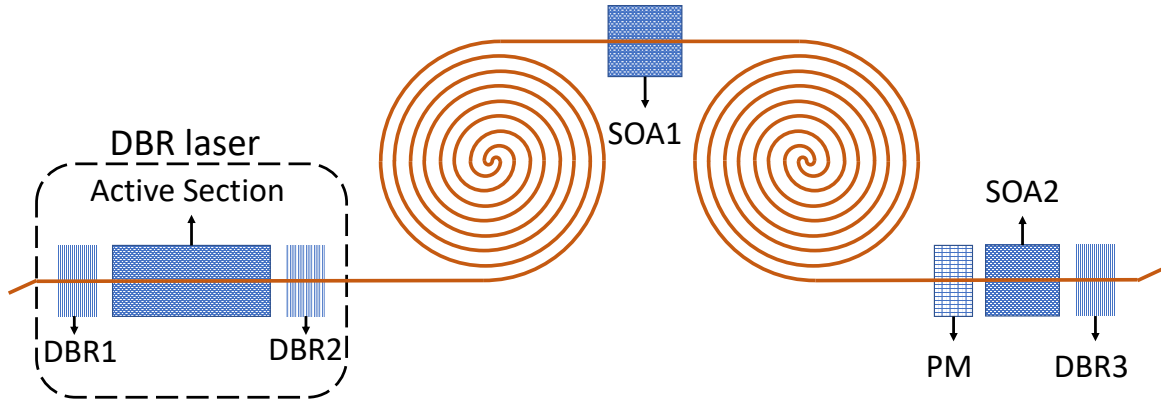


Figure 1. Schematic depiction of our InP-based photonic integrated circuit (PIC). The PIC consists of a laser structure followed by a delay line of 5.4 cm. DBR: Distributed Bragg Reflector, SOA: Semiconductor Optical Amplifier, PM: Phase Modulator.

The device covers the whole 6mm width of the chip and has one optical input/output port on each side. The ports are angled with respect to the chip edge to minimize reflection. We employed lensed fibers to send optical signals in/out of these ports and a total of five electrical DC probes to operate the device. The first probe (I_{DBR1}) was placed on the left DBR of the laser structure, in order to tune the spectral output of the laser. The second probe (I_L) acted to supply the pump current to the laser. The following two probes (I_{SOA1} , I_{SOA2}) supplied current to the SOAs along the feedback line and the last probe (I_{DBR3}) tuned the reflection spectrum of the DBR at the end of the feedback line. The active and SOA sections could be pumped up to a current of 40 mA, whereas the tuning currents of the DBRs could only be driven up to 10 mA.

The DBR laser has a threshold current of 15 mA. The free running lasing wavelength is centered at 1546.91 nm. In our setup, the on-chip laser can lock on the injection at the free running lasing wavelength or one of the side-modes, depending on the injected wavelength. It turned out that the RC performance is best when the injected field's wavelength is close to a side mode. Targeting the side mode allows for a higher injected power as the reflection of DBR1 is lower at the wavelength of the side-mode. Furthermore, DBR2 has a higher transmission for side modes than for the free running lasing wavelength. Injection locking on the side-mode is achieved at a wavelength of 1549.60 nm and the following DC probes configuration: $I_{DBR1} = 8.28$ mA, $I_{DBR3} = 1$ mA, and $I_L = I_{SOA1} = I_{SOA2} = 40$ mA. The on-chip spectral parameters are not changed hereafter, meaning that the current supply to the two DBRs is not changed throughout the paper.

To test the RC performance of the laser integrated with a feedback loop, the setup shown in Fig. 2 is used. We use a wavelength tuneable CW laser to create the optical injection signal. The wavelength of this laser is set close to 1549.6 nm, but we still allow for a small detuning between the injection wavelength and the wavelength of the targeted side-mode of the laser. The CW light beam of the tunable laser is modulated using a 40GHz Mach-Zehnder modulator (iXblue MX-LN-40). This modulator is driven electrically by a 25GHz Arbitrary Waveform Generator (Keysight M8195A) set at a sample speed of 60 GSa/s.

We employ the time-multiplexing scheme, where the duration of one data sample matches the 1170 ps delay time. Note that there have been numerical and experimental studies, where the duration of a data sample does not match the delay time.^{7,20} We, however, do not target this working regime.

Any input data sample u_i , in our case originating from a discrete timeseries, is held constant for the duration of one delay time τ . We then multiply this piecewise constant stream $U(t)$ with a piecewise constant mask $M(t)$ (that is periodic with a period of τ) to obtain the masked input stream $J(t)$. The piecewise constant levels of stream $J(t)$ define the position of the virtual nodes equally spread over the delay line. It has been shown numerically²¹ that the node separation, when using a semiconductor laser with delayed feedback, can be as short as a few tens of ps. As the sample rate of the AWG is set to 60 GSa/s, we use three AWG samples to define one mask node, leading to a mask node separation of $\theta_M = 50$ ps such that 23 nodes fit within one round-trip in the delay loop. We thus generate a random mask with $N_M = 23$ mask nodes with three possible values $[0, 0.5, 1]$.

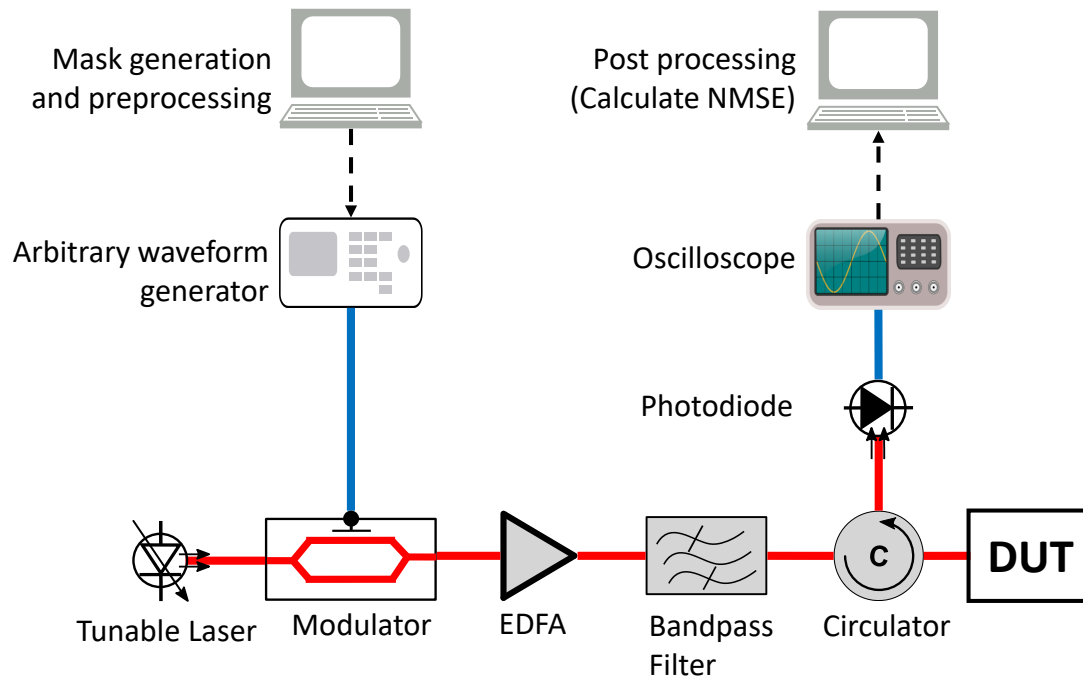


Figure 2. Schematic depiction of the setup used to measure the performance of our integrated delay-based reservoir computer. The device under test (DUT) is the PIC shown in Fig. 1

In our case the length of the mask is 20 ps shorter than the delay time, which is hard to match in practice. We believe this desynchronization will not adversely affect the performance of the RC scheme, since the mismatch is smaller than the node separation and we can accurately split the reservoir output in the readout layer.²²

The modulated optical signal is next amplified in Fig. 2 using an Erbium doped fiber amplifier (Keopsys CEFA-C-BO-HP-B203). The broadband spontaneous emission noise, added to the optical signal by the amplifier, is removed by sending the light beam through an optical bandpass filter, that is centered around the injection signal's wavelength. The filtered signal is then fed into the laser using a circulator connected to a lensed fiber. The response of the laser is collected at the third port of the circulator and measured using an opto-electronic detector connected to a 63GHz real-time oscilloscope. The sampling rate of the oscilloscope was set to 40 GSa/s. This means that each mask node, with a duration of 50 ps, has 2 corresponding samples in the read-out signal.

We have studied the performance of a delay-based reservoir computer, which is designed on a photonic integrated chip. The integrated approach leads to a compact design as well as high computation speeds. We have studied the performance through the Santa-Fe timeseries benchmarking task.

With a conventional reservoir computing scheme, where the mask-imposed nodes coincide with the virtual nodes, we get a performance (best $NMSE = 0.135$) which is slightly worse than those found in other works ($NMSE$ around 0.1). However, we are working in different regimes. While previous works, such as,^{9,11,16,21} operate in sub- or near threshold regimes, we operate our laser at pump currents well above the threshold current. We achieve a significant speed up compared to others,^{6,9} who achieved speeds in the order of kSa/s and MSa/s respectively. The computation speed of our setup is 0.87 GSa/s, which is comparable to what Takano *et al.* achieved with additional pre- and post-processing steps.

We were able to improve the performance of the reservoir computer by using different post-processing routines. The first routine is using both readout samples within one mask-imposed node to form the output layer, unlike the conventional routine where we utilize one sample per mask-imposed node. The availability of extra states in the output layer, causes the reservoir computer to perform better. The extra states are not redundant in comparison with the rest, but rather enhance the state space. Since the mask-imposed node has a slightly longer

duration than the timescale of the laser, we get two different state values from the transient response on the input. The best performance we achieved here is $NMSE = 0.062$.

The second post-processing routine takes the reservoir output for a duration of two delay times. This way we have a richer state space to perform the task and furthermore have access to a longer temporal memory inside this state space, since the last two input data points are present in the two delay times. This post-processing routine has consistently been the best performing out of the three and reaches an $NMSE$ as low as 0.049.

We have seen that the best performance for Santa Fe timeseries prediction was found when we the injected signal's wavelength was close to a side-mode, with zero detuning between the injected wavelength and side-mode. We also observed that delay-based RC using semiconductor lasers can achieve very good performances at pump currents well above threshold, where most studies have focused on near-threshold operation. Lastly, we studied the memory capacity of our RC setup as the feedback in the setup is increased and we see a clear increase. Even when the SOAs in the delay line are turned off, we get a linear memory capacity around 8, which suggests that there is enough feedback already in the system without extra amplification.

2. TIME MULTIPLEXING FOR ISING MACHINES

Motivated by the exponentially increasing energy consumption of high-performance computing and the looming end of Moore's law, there has been a very active search for new non-von-Neumann computing architectures that are both faster and more energy efficient than conventional digital computers. Ising machines have emerged as a promising concept, that specializes in solving resource intensive optimization problems, such as route planning, crew scheduling, protein folding or training of neural networks. Ising machines solve these difficult problems by mapping the problem's cost function to a network of coupled Ising spins $\sigma_i = \{-1, +1\}$, whose energy is described by the Ising Hamiltonian

$$H_{Ising} = -\frac{1}{2} \sum_{ij} J_{ij} \sigma_i \sigma_j \quad (1)$$

By implementing this spin system with bistable analog oscillators, the natural tendency to evolve to its lowest energy configuration is then used to efficiently find optimal solutions at significantly improved speeds compared to digital computers. However, it is still a challenge to find suitable analog oscillators that provide both high analog bandwidths as well as low energy consumption. Quantum annealing hardware²³ and photonic Ising machine based on coupled lasers, SLMs,²⁴ degenerate optical parametric oscillators (DOPOs)^{25,26} and polariton condensates²⁷⁻²⁹ have emerged in recent years and demonstrated potential performance gains over digital hardware. Yet, these systems rely on complex physical systems to realize the Ising spins, which can result in large footprints and high energy consumption.^{30,31}

Optoelectronic oscillators³² (OEOs) are a promising alternative to these complex Ising machines. With their compact and inexpensive layout, they can be easily fabricated from off-the-shelf components or as integrated photonic circuits.³³ Furthermore, they utilize components which are also used in optical data communication and that yield high analog bandwidths of 40 GHz. Fig. 3a shows a schematic of an OEO used as an Ising machine.

The OEO consists of a laser diode, a Mach-Zehnder intensity modulator and a photodiode. The output of the photodiode is fed back into the RF input of the modulator to create a closed feedback loop. By removing the DC component of the photovoltage and adjusting the feedback gain and the bias voltage of the modulator, the OEO is driven into a symmetrically bistable configuration. In this configuration, the system possesses two stable fixed points $x_1^*, 2\}$ with $x_1^* = -x_2^*$ and an unstable trivial fixed point $x_0^* = 0$ that lies in between the stable fixed points. Fig. 3b shows the temporal dynamics of 100 isolated OEOs when the system is initialized in the trivial fixed point x_0^* . When the gain is high enough, the OEOs will bifurcate into one of the two stable fixed points with a corresponding probability of 50 percent. This binary behavior is exploited to implement Ising spins by associating the fixed points with the spin up and spin down configuration respectively. An isolated OEO can thus implement a single Ising spin. To implement large Ising models, a time-multiplexing approach as depicted in Fig. 3a is employed. Here, spins are sequentially circulated in the feedback line of a single OEO to implement a large number of spins. An FPGA in the feedback loop is used to multiplex the input to the

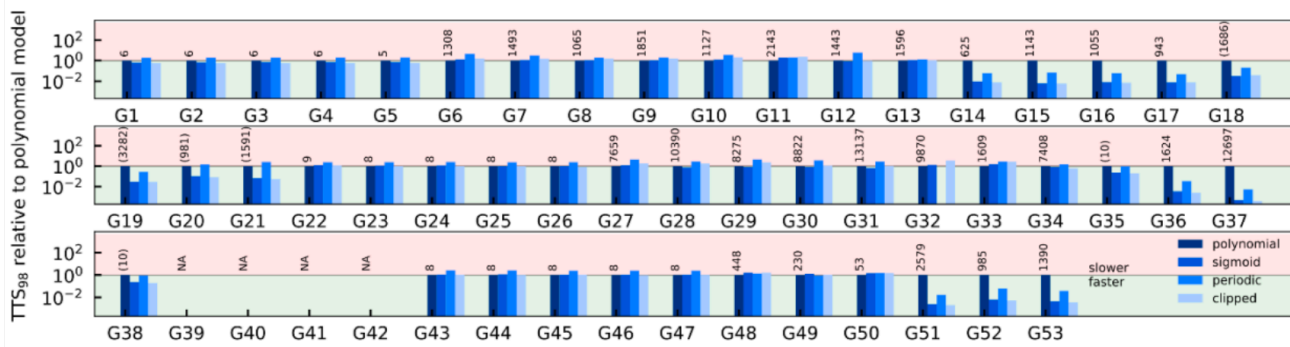


Figure 5. Time-to-solution (TTS) to reach 98 percent of the best known solution for the SparseSuite matrix collection of Ising machines with sigmoid, periodic and clipped transfer functions relative to Ising machines based on polynomial transfer functions

optimization problems. As a benchmark task, we consider MaxCut problems contained in the SuiteSparse matrix collection.

To assess the performance, we calculate the time-to-solution (TTS), which reflects the time required to reach a given solution with a probability of at least 99 percent. In Fig. 5, we assess the TTS to reach at least 98 percent of the best-known solution. The TTS is shown relative to the polynomial model to indicate the differences between the different types of Ising machines. We observe that for a large range of problems, all models achieve very similar TTSs, which indicates that they are equally capable of encoding and solving Ising models. This is to be expected since the different models have been shown to well approximate the polynomial model. However, for some specific hard instances, we can observe significant differences in the TTS. Compared to the polynomial model, the other models achieve speed-ups of up to three orders of magnitude. For these specific cases, we observe that the success rate for the polynomial model is significantly reduced, so that optimal solutions are found with a much lower probability.

We link these differences to the saturable nature of the different transfer functions. While the amplitude of the polynomial is unbound and grows continuously with the feedback gain, the transfer function for the other models saturates for large gain and thus limits the maximal amplitude. We find that this saturation ensures that the analog amplitude for each spin is narrowly distributed around the fixed points, while the amplitudes are broadly distributed for the polynomial model. It is well known that such broad amplitude inhomogeneity leads to an incorrect mapping to the Ising Hamiltonian, which in turn leads to convergence to suboptimal solutions.³⁶ We observe a direct correspondence between the amount of inhomogeneity and the success rate, so that the periodic, sigmoid and clipped transfer functions achieve higher success rates. This indicates that OEO-based Ising machines, along with Ising machines based on other saturable transfer functions, have an inherent advantage over DOPO-based Ising machines for specific problems. Furthermore, this demonstrates how the transfer function can be used as an efficient way of mitigating amplitude inhomogeneity, which is still an essential challenge for analog Ising machines.

ACKNOWLEDGEMENTS

We would like to acknowledge funding from the Research Foundation Flanders (FWO) through grants G028618N, G024715N, G029519N and G006020N, from the EU Horizon 2020 PHRESCO Grant (688579) and the EU Horizon 2020 Fun-COMP Grant (780848). Finally, we would like to thank BELSPO for funding through IAP P7-35 program Photonics@be, the Hercules Foundation and the Research Council of the VUB.

REFERENCES

- [1] Krizhevsky, A., Sutskever, I., and Hinton, G. E., "Imagenet classification with deep convolutional neural networks," in *[Advances in neural information processing systems]*, 1097–1105 (2012).

- [2] Van der Sande, G., Brunner, D., and Soriano, M. C., “Advances in photonic reservoir computing,” *Nanophotonics* **6**(3), 561–576 (2017).
- [3] Brunner, D. and Fischer, I., “Reconfigurable semiconductor laser networks based on diffractive coupling,” *Optics Letters* **40**(16), 3854–3857 (2015).
- [4] Schumacher, J., Toutounji, H., and Pipa, G., “An introduction to delay-coupled reservoir computing,” in [*Artificial Neural Networks*], 63–90, Springer (2015).
- [5] Soriano, M. C., Ortin, S., Keuninckx, L., Appeltant, L., Danckaert, J., Pesquera, L., and Van der Sande, G., “Delay-Based Reservoir Computing: Noise Effects in a Combined Analog and Digital Implementation,” *IEEE TRANSACTIONS ON NEURAL NETWORKS AND LEARNING SYSTEMS* **26**, 388–393 (FEB 2015).
- [6] Paquot, Y., Dambre, J., Schrauwen, B., Haelterman, M., and Massar, S., “Reservoir computing: a photonic neural network for information processing,” in [*SPIE Photonics Europe*], 77280B–77280B, International Society for Optics and Photonics (2010).
- [7] Paquot, Y., Duport, F., Smerieri, A., Dambre, J., Schrauwen, B., Haelterman, M., and Massar, S., “Opto-electronic reservoir computing,” *Scientific Reports* **2** (2012).
- [8] Pauwels, J., Verschaffelt, G., Massar, S., and Van der Sande, G., “Distributed Kerr Non-linearity in a Coherent All-Optical Fiber-Ring Reservoir Computer,” *FRONTIERS IN PHYSICS* **7** (OCT 3 2019).
- [9] Brunner, D., Soriano, M. C., Mirasso, C. R., and Fischer, I., “Parallel photonic information processing at gigabyte per second data rates using transient states,” *Nature Communications* **4**, 1364 (2013).
- [10] Hicke, K., Escalona-Morán, M. A., Brunner, D., Soriano, M. C., Fischer, I., and Mirasso, C. R., “Information processing using transient dynamics of semiconductor lasers subject to delayed feedback,” *IEEE Journal of Selected Topics in Quantum Electronics* **19**(4), 1501610–1501610 (2013).
- [11] Takano, K., Sugano, C., Inubushi, M., Yoshimura, K., Sunada, S., Kanno, K., and Uchida, A., “Compact reservoir computing with a photonic integrated circuit,” *Optics Express* **26**(22), 29424–29439 (2018).
- [12] Nguimdo, R. M., Verschaffelt, G., Danckaert, J., and Van der Sande, G., “Simultaneous computation of two independent tasks using reservoir computing based on a single photonic nonlinear node with optical feedback,” *IEEE Transactions on Neural Networks and Learning Systems* **26**(12), 3301–3307 (2015).
- [13] Vatin, J., Rontani, D., and Sciamanna, M., “Enhanced performance of a reservoir computer using polarization dynamics in vcsels,” *Optics Letters* **43**(18), 4497–4500 (2018).
- [14] Hurtado, A., Schires, K., Henning, I. D., and Adams, M., “Investigation of vertical cavity surface emitting laser dynamics for neuromorphic photonic systems,” *Applied Physics Letters* **100**(10), 103703 (2012).
- [15] Harkhoe, K. and Van der Sande, G., “Delay-Based Reservoir Computing Using Multimode Semiconductor Lasers: Exploiting the Rich Carrier Dynamics,” *IEEE JOURNAL OF SELECTED TOPICS IN QUANTUM ELECTRONICS* **25** (NOV-DEC 2019).
- [16] Bueno, J., Brunner, D., Soriano, M. C., and Fischer, I., “Conditions for reservoir computing performance using semiconductor lasers with delayed optical feedback,” *Optics Express* **25**(3), 2401–2412 (2017).
- [17] Kuriki, Y., Nakayama, J., Takano, K., and Uchida, A., “Impact of input mask signals on delay-based photonic reservoir computing with semiconductor lasers,” *Opt. Express* **26**, 5777–5788 (Mar 2018).
- [18] Leijtens, X., “Jeppix: the platform for indium phosphide-based photonics,” *IET optoelectronics* **5**(5), 202–206 (2011).
- [19] Nguimdo, R. M., Verschaffelt, G., Danckaert, J., and Van der Sande, G., “Reducing the phase sensitivity of laser-based optical reservoir computing systems,” *OPTICS EXPRESS* **24**, 1238–1252 (JAN 25 2016).
- [20] Duport, F., Smerieri, A., Akrouf, A., Haelterman, M., and Massar, S., “Fully analogue photonic reservoir computer,” *Scientific Reports* **6**, 22381 (2016).
- [21] Nguimdo, R. M., Verschaffelt, G., Danckaert, J., and Van der Sande, G., “Fast photonic information processing using semiconductor lasers with delayed optical feedback: role of phase dynamics,” *Optics Express* **22**(7), 8672–8686 (2014).
- [22] Harkhoe, K. and Van der Sande, G., “Task-independent computational abilities of semiconductor lasers with delayed optical feedback for reservoir computing,” *Photonics* **6**(4) (2019).

- [23] Johnson, M. W., Amin, M. H. S., Gildert, S., Lanting, T., Hamze, F., Dickson, N., Harris, R., Berkley, A. J., Johansson, J., Bunyk, P., Chapple, E. M., Enderud, C., Hilton, J. P., Karimi, K., Ladizinsky, E., Ladizinsky, N., Oh, T., Perminov, I., Rich, C., Thom, M. C., Tolkacheva, E., Truncik, C. J. S., Uchaikin, S., Wang, J., Wilson, B., and Rose, G., “Quantum annealing with manufactured spins,” *Nature* **473**(7346), 194–198 (2011).
- [24] Pierangeli, D., Marcucci, G., and Conti, C., “Large-Scale Photonic Ising Machine by Spatial Light Modulation,” *Physical Review Letters* **122**(21), 1–6 (2019).
- [25] Okawachi, Y., Yu, M., Jang, J. K., Ji, X., Zhao, Y., Kim, B. Y., Lipson, M., and Gaeta, A. L., “Demonstration of chip-based coupled degenerate optical parametric oscillators for realizing a nanophotonic spin-glass,” *Nature Communications* **11**, 4119 (dec 2020).
- [26] Marandi, A., Wang, Z., Takata, K., Byer, R. L., and Yamamoto, Y., “Network of time-multiplexed optical parametric oscillators as a coherent Ising machine,” *Nature Photonics* **8**(12), 937–942 (2014).
- [27] Utsunomiya, S., Takata, K., and Yamamoto, Y., “Mapping of Ising models onto injection-locked laser systems,” *Optics express* **19**(19), 18091 (2011).
- [28] Wang, Z., Marandi, A., Wen, K., Byer, R. L., and Yamamoto, Y., “Coherent Ising machine based on degenerate optical parametric oscillators,” *Phys. Rev. A* **88**(063853), 1–9 (2013).
- [29] Berloff, N. G., Silva, M., Kalinin, K., Askitopoulos, A., Töpfer, J. D., Cilibrizzi, P., Langbein, W., and Lagoudakis, P. G., “Realizing the classical XY Hamiltonian in polariton simulators,” *Nature Materials* **16**, 1120–1126 (nov 2017).
- [30] Takesue, H., Inagaki, T., Inaba, K., Ikuta, T., and Honjo, T., “Large-scale Coherent Ising Machine,” *Journal of the Physical Society of Japan* **88**(6), 061014 (2019).
- [31] Cai, F., Kumar, S., Van Vaerenbergh, T., Sheng, X., Liu, R., Li, C., Liu, Z., Foltin, M., Yu, S., Xia, Q., Yang, J. J., Beausoleil, R., Lu, W. D., and Strachan, J. P., “Power-efficient combinatorial optimization using intrinsic noise in memristor Hopfield neural networks,” *Nature Electronics* **3**, 409–418 (jul 2020).
- [32] Chembo, Y. K., Brunner, D., Jacquot, M., and Larger, L., “Optoelectronic oscillators with time-delayed feedback,” *Reviews of Modern Physics* **91**, 035006 (sep 2019).
- [33] Böhm, F., Verschaffelt, G., and Van der Sande, G., “A poor man’s coherent Ising machine based on optoelectronic feedback systems for solving optimization problems,” *Nature Communications* **10**, 3538 (dec 2019).
- [34] McMahon, P. L., Marandi, A., Haribara, Y., Hamerly, R., Langrock, C., Tamate, S., Inagaki, T., Takesue, H., Utsunomiya, S., Aihara, K., Byer, R. L., Fejer, M. M., Mabuchi, H., and Yamamoto, Y., “A fully programmable 100-spin coherent Ising machine with all-to-all connections,” *Science* **354**(6312), 614–617 (2016).
- [35] Hamerly, R., Inagaki, T., McMahon, P. L., Venturelli, D., Marandi, A., Onodera, T., Ng, E., Langrock, C., Inaba, K., Honjo, T., Enbutsu, K., Umeki, T., Kasahara, R., Utsunomiya, S., Kako, S., Kawarabayashi, K.-i., Byer, R. L., Fejer, M. M., Mabuchi, H., Englund, D., Rieffel, E., Takesue, H., and Yamamoto, Y., “Experimental investigation of performance differences between coherent Ising machines and a quantum annealer,” *Science Advances* **5**, eaau0823 (may 2019).
- [36] Leleu, T., Yamamoto, Y., McMahon, P. L., and Aihara, K., “Destabilization of Local Minima in Analog Spin Systems by Correction of Amplitude Heterogeneity,” *Physical Review Letters* **122**, 040607 (feb 2019).